The *n*-butanol fraction of *Naematoloma sublateritium* suppresses the inflammatory response through downregulation of NF-κB in human endothelial cells

YU RAN LEE[1*], KI MO KIM[2*], BYEONG HWA JEON[1], JONG WOON CHOI[3] and SUNGA CHOI[1]

[1]Department of Physiology, School of Medicine, Chungnam National University, Daejeon 301747; [2]Traditional Korean Medicine-Based Herbal Drug Research Group, Herbal Medicine Research Division, Korea Institute of Oriental Medicine (KIOM), Daejeon 305811; [3]Gangwon Forest Research Institute, Chuncheon, Gangwon-do 200140, Republic of Korea

Received December 1, 2011; Accepted January 24, 2012

DOI: 10.3892/ijmm.2012.914

Abstract. *Naematoloma sublateritium* (Fr.) P. Karst is a chestnut mushroom that is currently a popular edible fungus in the USA, Japan, China and Korea. Although its therapeutic potential in the treatment of diseases has been demonstrated, the pharmacological effect of *N. sublateritium* (NS) has been poorly studied. In the present study, we demonstrate for the first time that NS suppresses TNF-α-induced inflammatory response in human umbilical vein endothelial cells. The *n*-butanol fraction of NS (BFNS) inhibited TNF-α-induced monocyte adhesion to endothelial cells in a dose-dependent manner. The anti-adhesive activity of BFNS correlated with suppressed expression of vascular cell adhesion molecule-1, intercellular adhesion molecule-1, monocyte chemoattractant protein-1 and interleukin-8 at both the mRNA and protein levels. In addition, BFNS dose-dependently decreased the expression of inducible nitrogen oxygen synthase (iNOS) and cyclooxygenase-2 (COX-2). Notably, BFNS significantly regulated the nuclear factor (NF)-κB transcriptional activity that was activated by TNF-α stimulation. When considered together, these results suggest that BFNS inhibits the expression of TNF-α-induced adhesion molecules in addition to regulating the iNOS/COX-2 pathways through the modulation of NF-κB in endothelial cells. In conclusion, we propose that BFNS may be a potential therapeutic agent against vascular inflammation, such as atherosclerosis.

Correspondence to: Dr Sunga Choi, Department of Physiology, School of Medicine, Chungnam National University, 55 Munhwa-ro, Jung-gu, Daejeon 301747, Republic of Korea
E-mail: sachoi@cnu.ac.kr

*Contributed equally

Key words: *Naematoloma sublateritium*, *n*-butanol fraction of *Naematoloma sublateritium*, NF-κB, inflammation, endothelial cells, adhesion molecules

Introduction

Atherosclerosis, a cardiovascular disease, is a leading cause of death worldwide and is the result of a complicated inflammatory processes on the inner wall of large blood vessels. Immune responses can cause vascular endothelial dysfunctions that eventually disturb blood flow (1). In the early pathogenesis of atherosclerosis, the endothelium is activated by a variety of relevant stimuli, including oxidized lipids, cytokines, or signaling molecules such as endotoxins, and viruses, subsequently expressing specific adhesion receptors that enhance mononuclear cell recruitment into the vessel wall (2,3).

The immune reactions in atherosclerotic lesions are mediated by nitric oxide (NO) and cyclooxygenase-2 (COX-2) (4). In the physiological function of the endothelium, NO production is required to inhibit monocyte adhesion and smooth muscle cell chemotaxis and proliferation (5). However, high levels of NO, which are produced by inducible NO synthase (iNOS) in response to stimuli, induce subsequent inflammatory reactions, thus contributing to the progression of atherosclerosis (6). COX-2 has also been associated with pro-atherogenic reactions, generating lipid mediators of inflammation, such as prostaglandin E_2 (PGE_2) (7).

Epidemiological data continue to support the premise that dietary intake of natural products may improve vascular endothelial dysfunction in both *in vivo* and *in vitro* atherosclerotic models (8,9). For example, popular and edible mushrooms have been traditionally used to maintain health, and their components have been used in the prevention and treatment of diseases in many countries, including Korea. The *n*-butanol fraction of *Phellinus linteus* was effective in eliciting anti-inflammatory activity in RAW264.7 macrophages, inhibiting the production of NO and PGE_2 (10). *Cordyceps spp.*, whose main chemical constituent is cordycepin, have also been demonstrated to confer anti-inflammatory effects. Won *et al* reported that cordycepin attenuated neointimal formation by inhibiting reactive oxygen species (ROS)-mediated responses in vascular smooth muscle cells in rats (11). Moreover, some studies have reported that the natural component specifically inhibited the transcriptional activity in the cytokine-stimulated pro-inflammatory response (12,13). Two flavonoids, kaempferol

and quercetin, individually modulate pro-inflammatory genes and block nuclear factor-κB (NF-κB) and activator protein-1, respectively (14).

Naematoloma sublateritium (Fr.) P. Karst, a chestnut mushroom, grows on hardwood stumps and logs. Some studies have reported the biosynthesis of a human Ras-farnesyl transferase inhibitor, clavaric acid, and the antitumoral activity of *Hypholoma sublateritium* (15-17). However, the biological activities of *N. sublateritium* (NS) have been poorly studied. Our previous study revealed that NS has antioxidative and antitumoral activity. We extended this research and demonstrate for the first time that NS also has an anti-inflammatory effect on TNF-α-stimulated human umbilical vein cells (HUVECs). In the present study, we used an *n*-butanol fraction from NS (BFNS) to gain insight into its anti-inflammatory activity in TNF-α-stimulated endothelial cells. It was shown that BFNS could potentially suppress the expression of adhesion molecules and iNOS/COX-2 proteins by inhibiting NF-κB activation.

Materials and methods

Materials. HUVECs and monocyte U937 cells were obtained from Clonetics (Walkersville, MD, USA) and the American Type Culture Collection (#CCL-2, Rockville, MD, USA), respectively. Endothelial growth medium (EGM2), DMEM, fetal bovine serum (FBS), and antibiotics were purchased from Gibco (Grand Island, NY, USA). Human TNF-α was purchased from Sigma (St. Louis, MO, USA). Antibodies against vascular cell adhesion molecule (VCAM-1), intercellular adhesion molecule-1 (ICAM-1), endothelial-selectin (E-selectin), tubulin, and iNOS and β-actin were obtained from Santa Cruz Biotechnology (Santa Cruz, CA, USA) and Sigma, respectively. Monoclonal antibodies against iNOS, COX-2, and NF-κB were purchased from BD Transduction Laboratories (Lexington, KY, USA). Antibodies against COX-2 and PARP were obtained from Cell Signaling Technology (Beverly, MA) and Biomol (Plymouth Meeting, PA).

Preparation of the BFNS. Fruiting bodies of NS were obtained and authenticated by Dr Choi in the Gangwon Forest Research Institute (GFRI, Chuncheon, Korea). A voucher specimen (GFRI-NS-01) was deposited in the entomopathogenic fungal culture collection of the GFRI. The fruiting bodies were dried at 50˚C, crushed in a blender, and the crude powder was extracted with ethanol at 70˚C for 3 h according to a previous report, producing a 14.6% yield (10). The extract was evaporated at 60˚C under pressure and resuspended in distilled water. The ethanolic extract was sequentially fractionated with equal volumes of hexane, dichloromethane, *n*-butanol and ethyl acetate. Each fraction was concentrated on a rotary evaporator under reduced pressure and passed through a 0.2 μm filter paper for conservation. The fractions were dried again with a freeze-drier and stored at -20˚C.

HPLC analysis of the BFNS. Each fraction was dissolved in 2 ml DMSO before high performance liquid chromatography (HPLC) analysis (WellChrom HPLC-pump K-1001, WellChrom fast scanning spectrophotometer K-2600, and 4-channel degasser K-500) was carried out. HPLC separation was performed on a Gemini 5 μm C_{18} 110A column (30x50 mm; Phenomenex, Inc., Torrance, CA). The HPLC mobile phase was H_2O with 0.1% CF_3CO_2H (v/v) for solvent A and CH_3CN with 0.08% CF_3CO_2H (v/v) for solvent B; the gradient condition was as follows: 0-5 min, 40% solvent B; 5-15 min, 40-60% solvent B; and 15-25 min, 60% solvent B. The flow rate was 1 ml/min and all samples were injected in volumes of 20 μl. A UV/VIS detector was used to measure the absorbances at 278, 335, 400, and 520 nm.

Cell culture and cell viability assay. HUVECs were grown and maintained in EGM2 and used between passages 3 and 6. Suspended cultures of U937 cells were maintained in DMEM supplemented with 10% (v/v) FBS and antibiotics. Each cell line was incubated in an atmosphere of 95% air and 5% CO_2 at 37˚C. The effect of NS fractions on HUVEC viability was measured with an automatic cell counter (ADAM-MC; Digital Bio, Seoul, Korea), which analyzed propidium iodide (PI) staining.

Monocyte-endothelial cell adhesion assay. The monocyte-endothelial cell adhesion assay was performed as described previously (18). Briefly, U937 cells were labeled with 2', 7'-bis-(2-carboxyethyl)-5-(and-6)-carboxy-fluorescein acetoxymethyl ester (BCECF-AM) for the quantitative adhesion assay. $1x10^7$ labeled U937 cells were incubated with 1 μM BCECF-AM in RPMI-1640 medium for 30 min at 37˚C. HUVECs ($3x10^4$) were seeded in 96-well plates to reach confluent monolayers and treated with the BFNS in a concentration-dependent manner in EGM2 medium. The cells were subsequently treated with 15 ng/ml TNF-α for 18 h before labeled monocytes were added. After washing out the unbound U937 cells for 3 times, monocyte adhesion was measured by fluorescent intensity using Fluoroskan (Thermo Scientific). Wells containing HUVECs alone were used as blanks.

Semi-quantitative reverse transcription-PCR for adhesion molecules and cytokines. TNF-α-stimulated HUVECs were treated with DMSO (control) or BFNS at the indicated concentrations and then RNA was extracted using the BCP Phase Separation Reagent (MRC Inc., Cincinnati, OH). cDNA was synthesized by reverse transcription (RT) using a Maxime RT PreMix kit containing oligo (dT) primers from Intron Biotechnology (Seoul, Korea). The PCR exponential phase was determined between 22-30 cycles to allow semi-quantitative comparisons of the target. cDNAs were prepared with 1 master mix (Intron Biotechnology) containing 2 μl RT transcript, reaction buffer, 30 pM of primer, and 2.5 mM each dNTP and Taq polymerase (2.5 units). The primers and PCR conditions are listed in Table I. PCR products were electrophoresed on a 1% agarose gel and visualized under ultraviolet light after ethidium bromide staining.

Immunoblotting. Cells were treated with the BFNS at the specified concentrations and lysed, as described previously (18). The cell lysate was cleared by centrifugation at 12,000 x g for 20 min, and the supernatant was used for immunoblotting. Proteins were resolved on SDS-PAGE and transferred onto a PVDF membrane. Immunoblotting was performed using anti-VCAM-1, ICAM-1, and E-selectin and the band intensity was quantified using a densitometer followed by normalization to the density of β-actin.

Table I. PCR primers.

Target genes		Primer sequences	Size (bp)	Annealing temperature (˚C)	Cycles
VCAM-1	Sense	ATGCCTGGGAAGATGGTCGTGA	762	65	30
	Antisense	TGGAGCTGGTAGACCCTCGCTG			
ICAM-1	Sense	CAGTGACCATCTACAGCTTTCCG	547	65	30
	Antisense	GCTGCTACCACAGTGATGATGACAA			
COX-2	Sense	GGTCTGGTGCCTGGTCTGATGATG	724	65	30
	Antisense	GTCCTTTCAAGGAGAATGGTGC			
E-selectin	Sense	ATCATCCTGCAACTTCACC	345	55	30
	Antisense	ACACCTCACCAAACCCTTC			
IL-8	Sense	AAACCACCGGAAGGAACCAT	156	60	30
	Antisense	CCTTCACACAGAGCTGCAGAA			
MCP-1	Sense	CAGCCAGATGCAATCAATGC	302	60	30
	Antisense	GTGGTCCATGGAATCCTGAA			
β-actin	Sense	AGCAGAGAATGGAAAGTCAAA	266	55	30
	Antisense	ATGCTGCTTACATGTCTCGAT			

The number of cycles of β-actin as an internal control were adjusted to that of each target gene.

Preparation of nuclear and cytosolic fractions. Nuclear and cytosolic fractions from the control (DMSO) and BFNS-treated HUVECs were prepared using a nuclear extraction kit from Pierce (Rockford, IL, USA) according to the manufacturer's instructions. Briefly, the cells were lysed and centrifuged at 15,000 x g for 3 min. The supernatant (cytosolic fraction) and nuclear pellet were collected. The nuclear pellet was resuspended in nuclear buffer (20 mM HEPES, pH 7.9, 0.4 M NaCl, 1 mM EDTA, 10% glycerol, 1 mM DTT, and protease inhibitors), vortexed, passed (15-20 times) through a 27 gauge needle, and centrifuged at 15,000 x g for 5 min. The supernatant fraction was collected and used for immunoblotting of p65 NF-κB.

Immunocytochemistry of NF-κB. HUVECs were cultured on coverslips, followed by treatment with DMSO (control) or 50, 100, or 200 μg/ml BFNS for 6 and 12 h and stimulation with TNF-α. After washing with PBS, cells were fixed with 4% paraformaldehyde and permeabilized with 0.1% Triton X-100. The cells were incubated with normal goat serum (1:20 dilution) in PBS for 45 min. Subsequently, the cells were treated with anti-p65 NF-κB antibody (1:500 dilution) for 2 h. The cells were washed with PBS and incubated with Alexa Fluor 488-conjugated secondary antibody (1:1,000 dilution; Molecular Probes) for 1 h. After washing, cells were counterstained with PI for 1 min. The cells were visualized under a fluorescence microscope (Axiophot; Carl Zeiss, Germany).

Transient transfection and luciferase reporter assay. HUVECs were plated at a density of $2x10^5$ cells/well in 12-well plates, allowed to attach overnight, and transfected with 0.8 μg of total plasmid containing 0.78 μg/well of NF-κB-luciferase reporter plasmid and 20 ng/well of pCMV-pRL internal control vector (Promega) using lipofectamine (Invitrogen). After transfection, the cells were treated with BFNS for the desired period, followed by stimulation with TNF-α. Then, the cells were washed with ice-cold PBS and harvested in reporter lysis buffer. After centrifugation, 20 μl of supernatant fraction were used for measurement of dual luciferase activity (Promega) using a luminometer. The luciferase activity was normalized against protein concentration and expressed as relative luciferase activity (a ratio of firefly luciferase to *Renilla* luciferase units).

Electrophoretic mobility shift assay for NF-κB. TNF-α stimulated HUVECs were treated with BFNS at the specified concentrations. Nuclear extracts were prepared as described above and 2 μg of nuclear protein were assembled with 10X Gel Shift Binding buffer (20% glycerol, 5 mM $MgCl_2$, 2.5 mM EDTA, 2.5 mM DTT, 250 mM NaCl, and 50 mM Tris-HCl), 0.25 mg/ml poly(dI)-poly(dC), and IRDye 700-labeled NF-κB oligonucleotide (LI-COR, Lincoln, NE). After incubation at room temperature for 30 min, the samples were loaded on a pre-run 8% polyacrylamide gel and electrophoresis was continued at 30 mA for 90 min. The signal was then detected and quantified with an Odyssey Infrared Imaging System (LI-COR).

Statistical analysis. Differences in the measured variables between the control and BFNS-treated groups were determined with a one-way analysis of variance (ANOVA) followed by Dunnett's or Bonferroni's test for multiple comparisons. A p-value of <0.05 was considered significant.

Results

HPLC analysis of the BFNS. The HPLC analysis chromatogram of the BFNS is shown in Fig. 1. It reveals major peaks at retention times of 23.7, 25.7, 27.1, 27.5, and 40.1 min at a wavelength of 278 nm. The peak profiles of the BFNS were

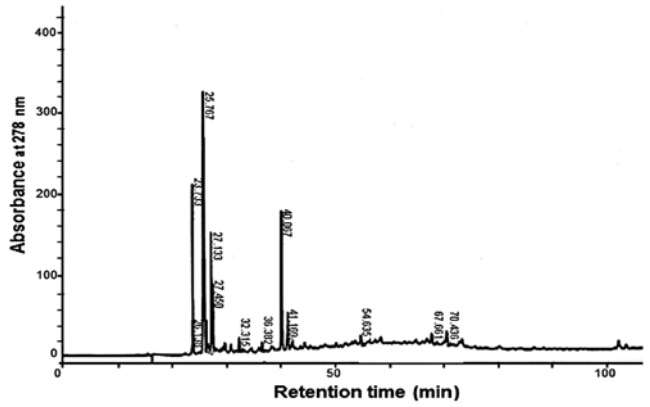

Figure 1. HPLC chromatogram (278 nm) of the *n*-butanol fraction (BFNS) from *Naematoloma sublateritium* (NS). The BFNS was analyzed with the KNAUER chromatography system. Elution solvents were distilled water and acetonitrile. The gradient step of the solvent was water to acetonitrile 1%/min and a Vydac C_{18} column was used.

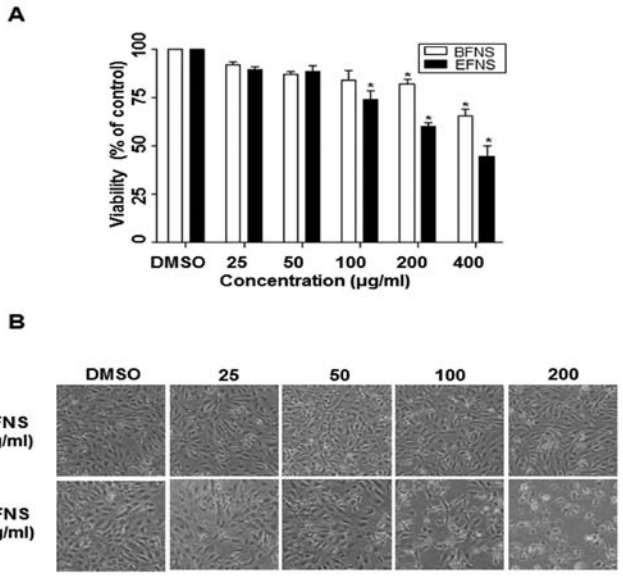

Figure 2. BFNS treatment does not cause reduction of viability at 25-100 μg/ml in human umbilical vein endothelial cells (HUVECs). (A) The effects of the BFNS and ethyl acetate fraction of NS (EFNS) on HUVEC viability were determined by propidium iodide (PI) staining and compared with DMSO-treated controls for 24 h at the indicated concentrations. (B) HUVEC morphological changes in response to the NS fractions were observed under phase-contrast microscopy (magnification, x200). Data are presented as means ± SEM (n=3). $^{*}p<0.05$, significantly different compared with control by a one-way ANOVA followed by Dunnett's test. Similar results were observed in replicate experiments.

observed at the early retention times, displaying polar characters. The HPLC profile of BFNS was similar to that of ethyl acetate fraction of NS (EFNS) (data not shown).

Effect of the BFNS on HUVEC viability. To investigate the potential effects of NS fractions on cell cytotoxicity, we examined the effect of BFNS and EFNS on HUVEC viability using PI staining. HUVEC viability was consistently maintained at the desired concentration although a slight decrease was detected at 200 μg/ml BFNS and 100 μg/ml EFNS, respectively (Fig. 2A). HUVECs demonstrated more than

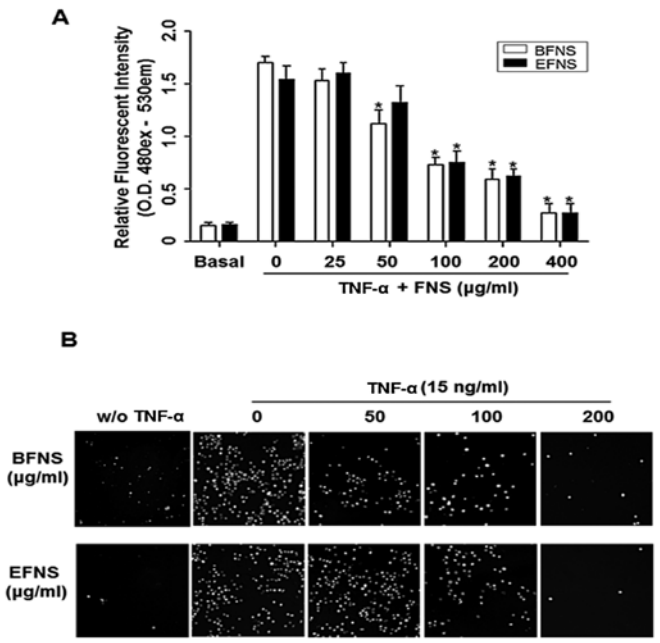

Figure 3. Quantitative adhesion assay of U937 monocytes to tumor necrosis factor-α (TNF-α)-stimulated HUVEC. (A) HUVECs were pretreated with BFNS or EFNS for 1 h followed by treatment with TNF-α for 18 h. Fluorescent-labeled U937 monocytes were added onto TNF-α-stimulated HUVECs and then incubated for 90 min. (A) The number of U937 cells adherent to the HUVECs was determined with a fluorometer. (B) Adherent U937 cells observed under a fluorescent microscope at x200 magnification. Data are representative of three independent experiments with similar results. Results are presented as means ± SEM (n=3). $^{*}p<0.05$, compared to the TNF-α-treated group as determined by one-way ANOVA followed by Dunnett's test.

85% viability at 200 μg/ml BFNS, indicating that it did not cause non-specific cytotoxicity (Fig. 2A). HUVEC viability by exposure to EFNS was affected in a concentration-dependent manner compared with that of BFNS-treated cells. These results were also observed under phase-contrast microscopy. As shown in Fig. 2B, HUVECs morphology was not affected by BFNS treatment even at 200 μg/ml compared to that of the EFNS-treated cells. Collectively, we determined that the BFNS preserved the viability of HUVECs relatively well, and concentrations of <200 μg/ml can be regarded as safe; as such, BFNS was used at concentrations of 100 μg/ml in subsequent experiments.

BFNS treatment inhibits TNF-α-induced monocyte adhesion. Next, we determined the functional significance of BFNS on the monocyte adhesion in endothelial cells. HUVECs were pretreated with BFNS and then incubated with TNF-α for 18 h. TNF-α-induced monocyte adhesion was markedly inhibited by BFNS in a concentration-dependent manner (Fig. 3A). For example, exposure to 100 μg/ml BFNS and EFNS resulted in a 57.1% and 48.7 % decrease, respectively, in monocyte adhesion relative to that in the DMSO-treated cells. The specific inhibitory action of BFNS was proven by a demonstration that BFNS itself did not affect monocyte adhesion (data not shown).

Fluorescent-labeled monocyte adhesion to TNF-α-stimulated endothelial cells was observed under fluorescent microscopy (Fig. 3B). The significant decrease of the fluorescence intensity induced by BFNS or EFNS treatment was concentration-dependent. The results indicate that these NS

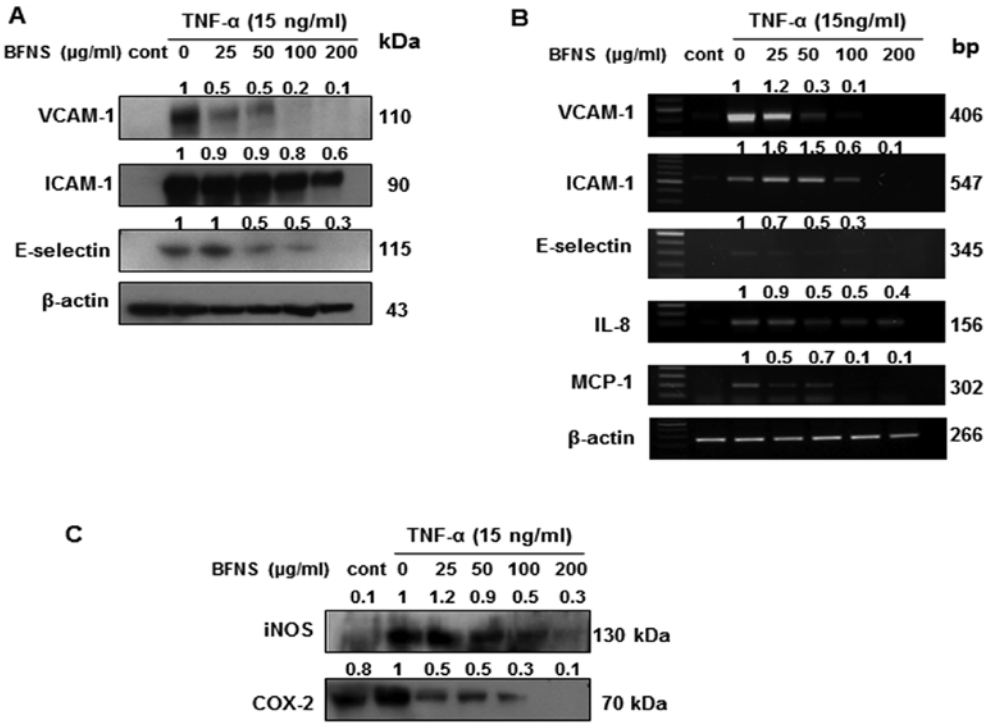

Figure 4. BFNS treatment resulted in alteration of adhesion molecule expression levels in TNF-α-stimulated HUVECs. (A) Immunoblotting for the adhesion molecules, VCAM-1, ICAM-1, and E-selectin using lysates from TNF-α-stimulated HUVECs treated with DMSO or BFNS at the indicated concentrations. Blots were stripped and reprobed with anti-actin antibody to correct for differences in protein loading. (B) Effects of BFNS on adhesion molecule transcript level as determined by quantitative RT-PCR. RT-PCR for β-actin was performed in parallel and displayed an equal amount of total RNA in the sample. (C) Protein levels of iNOS and COX-2 were determined using BFNS-treated cell lysates. Relative expression folds were calculated based on densitometric scanning data of each band.

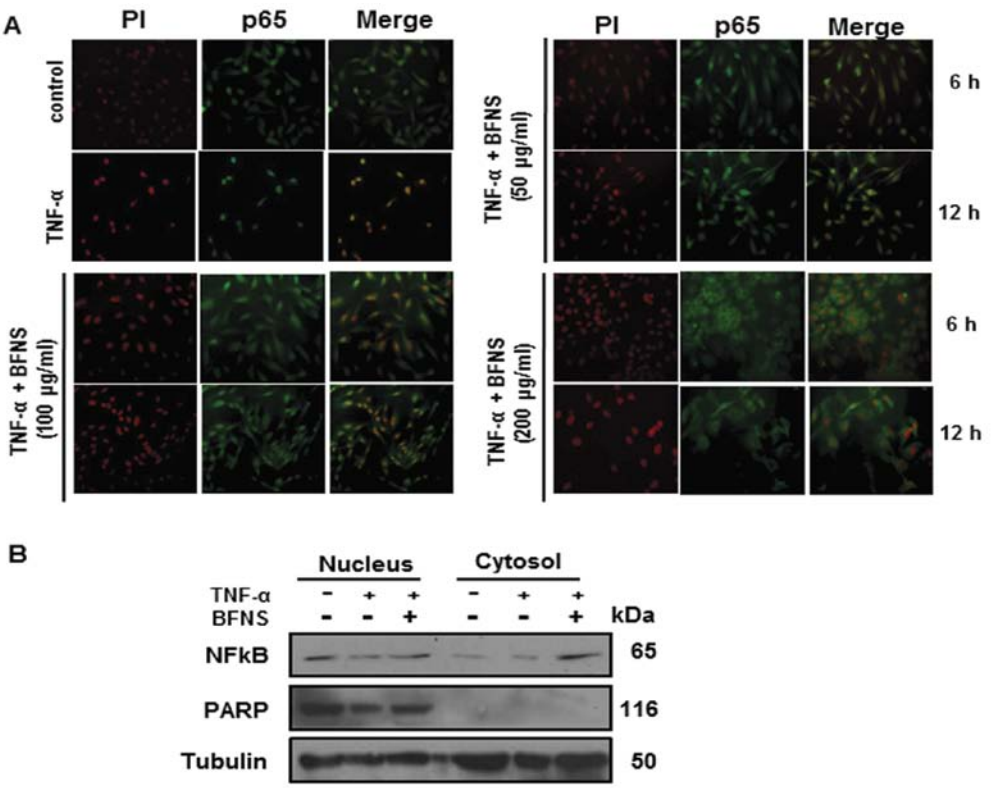

Figure 5. BFNS treatment caused translocation of nuclear factor-κB (NF-κB) from the nucleus to the cytosol in TNF-α-stimulated HUVECs. (A) Immunocytochemistry for analysis of p65 NF-κB localization following indicated exposure to DMSO or 50, 100 and 200 μg/ml BFNS in HUVECs. Green and red fluorescence indicate staining for p65 NF-κB and the nucleus, respectively. Images were merged to detect nucleus/cytosolic distribution of p65 NF-κB. (B) Immunoblotting for p65-NF-κB using nuclear and cytoplasmic fractions prepared from HUVECs following treatment with DMSO (control) or 100 μg/ml BFNS for 16 h. The blot was stripped and re-probed with anti-PARP and anti-α-tubulin antibody to ensure equal protein loading and to rule out cross-contamination of nuclear and cytoplasmic fractions.

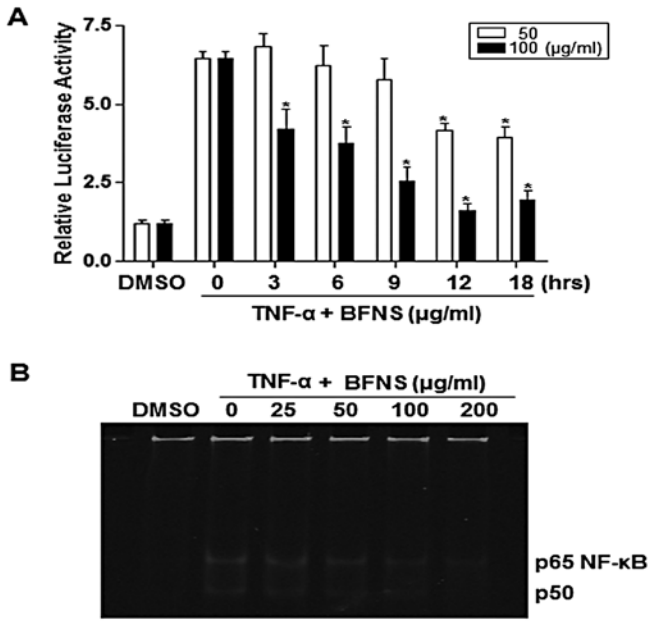

Figure 6. Treatment of BFNS significantly inhibited TNF-α-induced NF-κB activity. (A) Transcriptional activity of NF-κB in TNF-α-stimulated HUVECs following treatment with 50 or 100 μg/ml BFNS for the indicated times was determined by a luciferase reporter gene assay. Columns, mean (n=3); bars, SEM. *p<0.05, significantly different compared with the control by one-way ANOVA followed by Dunnett's test. Similar results were observed in replicate experiments. (B) A representative electrophoretic mobility shift assay (EMSA). HUVECs were incubated for 12 h with TNF-α and the BFNS at the indicated concentration. Nuclear extracts were incubated with IRDye-700-labeled NF-κB oligonucleotide.

fractions may be potential inhibitors of monocyte adherence to endothelial cell surfaces.

To further examine the BFNS-mediated monocyte adhesion, which was revealed by a decrease in fluorescent intensity (Fig. 3B), we determined the expression level of adhesion molecule on the surface of TNF-α-stimulated HUVECs. Exposure of HUVECs to TNF-α induced a significant up-regulation of adhesion molecules expression. Interestingly, BFNS significantly inhibited TNF-α-induced cell surface expression of VCAM-1, ICAM-1, and E-selectin in a concentration-dependent manner (Fig. 4A). For instance, when TNF-α-stimulated HUVECs were treated with 100 μg/ml BFNS for 18 h, expression levels of VCAM-1, ICAM-1 and E-selectin were significantly decreased to 0.2-, 0.8-, and 0.5-fold, respectively (Fig. 4A).

Additionally, we compared the levels of VCAM-1, ICAM-1, E-selectin, interleukin-8 (IL-8), and monocyte chemotactic protein-1 (MCP-1) mRNA in DMSO-or BFNS-treated cells. Representative semi-quantitative RT-PCR for adhesion molecules and cytokine mRNA using specific primer pairs are illustrated in Fig. 4B. Each mRNA level was quantified by densitometry of the cDNA bands and normalized with β-actin. Enhanced expressions VCAM-1, ICAM-1, E-selectin, IL-8 and MCP-1 mRNA by TNF-α stimulation were reduced by BFNS treatment in a statistically significant and dose-dependent manner (0.1-0.9-fold decrease over control). These RT-PCR results were well-correlated with those of the immunoblotting. Based on these results, it was confirmed that the 50% inhibition dose (ID_{50}) of the BFNS for monocyte adhesion was 100 μg/ml.

Also, as shown in Fig. 4C, stimulation of HUVECs with TNF-α caused a marked increase in iNOS and COX-2 expression. However, BFNS treatment evoked a significant and concentration-dependent decrease in iNOS and COX-2 at the protein level by 0.5- and 0.3-fold, respectively.

Effect of BFNS treatment on NF-κB localization and transcriptional activity. Regarding the regulation of adhesion molecules, cytokine, iNOS and COX-2 gene expression, we examined the activity of the NF-κB transcription factor in TNF-α stimulated HUVECs. We first performed immunocytochemistry to examine the effect of BFNS treatment on nuclear/cytoplasmic localization of p65 NF-κB. As shown in Fig. 5A, the p65 NF-κB (green fluorescence) immunostaining was evident in both the nucleus (red fluorescence) and cytoplasm in non-stimulated HUVECs compared with the mainly nuclear localization of p65 NF-κB in TNF-α stimulated cells. BFNS treatment significantly attenuated p65 NF-κB translocation and restricted it to the cytoplasm, indicating inhibition of its nuclear translocation (Fig. 5A). The cytoplasmic localization of p65 NF-κB in TNF-α-stimulated HUVECs was increased by BFNS in a concentration-dependent manner, being exhibited as early 6 h after BFNS treatment. Then, immunoblotting for p65 NF-κB was performed using nuclear fractions prepared from TNF-α-stimulated HUVECs treated with 100 μg/ml BFNS for 12 h. As seen in Fig. 5B, BFNS treatment caused an increase in the cytoplasmic level of p65 NF-κB compared with that of DMSO-treated cells.

Next, we examined whether BFNS treatment could decrease the transcriptional activity of NF-κB in TNF-α stimulated HUVECs using a luciferase reporter gene assay (Fig. 6A). As expected, a decrease in NF-κB transcriptional activity was observed in BFNS-treated HUVECs. Similarly to the expression of adhesion molecules and cytokines (Fig. 4), BFNS elicited downregulation of NF-κB transcriptional activity. The TNF-α-induced initial activation was followed by a 75.4% inhibition at the 12 h time point (Fig. 6A).

To evaluate NF-κB activation in the expression of TNF-α stimulated inflammation -associated molecules, we also investigated the change in NF-κB DNA-binding activity caused by BFNS treatment. As shown in Fig. 6B, DNA-binding activities of NF-κB significantly increased with TNF-α stimulation, and the activity significantly decreased in a concentration-dependent manner when cells were treated with BFNS.

Discussion

Natural products, which have been traditionally used in the treatment of inflammatory disease, are considered novel and effective biological agents (10-13). To develop novel therapeutic agents, it is important to investigate the mechanism regulating inflammatory signal reactions. The present study reports experimental evidence that BFNS plays an effective role with an IC_{50} of 100 μg/ml in the regulation of TNF-α-stimulated HUVECs. The following findings support the role of BFNS: a concentration-dependent decrease in adhesion molecule expression and monocyte adhesion in TNF-α-treated HUVECs, and the observed inhibition of NF-κB activation.

Consumption of natural products is associated with a lowered risk of cardiovascular disorder, including atheroscle-

rosis (19-21). There are many reports of the biological activity of natural agents. For example, curcumin inhibits monocyte adhesion by regulation of ROS, expression of adhesion molecules and inhibition of NF-κB activity. This regulation mediates leukocyte adherence in the process of leukocyte trafficking, inhibiting vascular inflammation (12). In the present study, BFNS and EFNS demonstrated inhibition of monocyte adhesion in TNF-α-stimulated endothelial cells and exhibited statistically significant anti-inflammatory activity in a dose-dependent manner. Treatment with 25-100 μg/ml BFNS did not affect the viability of HUVECs excluding cytotoxicity although exposure of EFNS caused 23.2% decreased viability at the 100 μg/ml concentration as observed with PI staining. BFNS relatively preserved the viability of HUVECs and was regarded as safe at concentrations <100 μg/ml, which inhibited U937 adhesion induced by TNF-α within the nontoxic range.

Monocyte adherence includes regulation of both secreted molecules such as the chemoattractant cytokines and surface-expressed, cell-adhesion molecules, in addition to immunoglobulin families in the process of monocyte trafficking (22-24). The upregulation of adhesion molecules, including VCAM-1 and ICAM-1 on the surface of the endothelium, is required for the firm adhesion of rolling monocytes. We found that VCAM-1, ICAM-1, E-selectin, MCP-1, and IL-8 expressions were attenuated by BFNS at both the mRNA and protein levels in TNF-α-stimulated HUVECs. These results indicate that the mechanism of anti-adhesion is at least in part related to downregulation of these proteins.

iNOS and COX-2, both inflammatory genes appear to be upregulated in cytokine-stimulated HUVECs, although less information exists on changes of their expression levels in endothelial cells (24). Under oxidative stress, high levels of NO, which are produced by iNOS in endothelial cells, may reflect the degree of vascular inflammation (6). COX-2 has also been implicated in the proatherogenic stages by the generation of lipid mediators, although some COX-2 inhibitors increase the risk of cardiovascular events (7). We observed that BFNS significantly suppressed TNF-α-induced iNOS and COX-2 protein expression. When considered together, these results clearly suggest that BFNS treatment of TNF-α-stimulated HUVECs induces significant inhibition of adhesion molecules, chemokine, iNOS, and COX-2 expression, indicating that regulation of mRNA and protein expression is one of the pathways by which the BFNS inhibits the adhesion of monocytes to endothelial cells. In addition, it is reasonable to suggest that BFNS attenuates the rolling, adhesion, and migration of monocytes through the endothelium to vascular smooth muscle cells, inhibiting the expression of adhesion molecules on HUVECs.

NF-κB is a ubiquitous protein transcription factor that plays an important role in the regulation of pro-inflammatory genes related to chronic diseases, including atherosclerosis. Many studies also suggest that the anti-inflammatory effect of natural products results from the inhibitory activity on NF-κB in various cell types leading to regulation of cytokines and adhesive molecules (13,25). In accordance with other reports on the regulation of the expression of adhesion molecules, we observed that p65 NF-κB was significantly activated and mainly localized within the nucleus in HUVECs subjected to TNF-α, while BFNS treatment repressed the translocation of p65 NF-κB. This was confirmed by immunoblotting of p65 NF-κB which demonstrated its localization in the cytoplasm after treatment with BFNS (Fig. 5). Furthermore, in TNF-α-stimulated HUVECs using a reporter gene assay, we found a time-dependent repression of p65 NF-κB transcriptional activity in response to 50 or 100 μg/ml BFNS. Accordingly, BFNS causes moderate inhibition of the p50/p65 NF-κB/DNA binding complexes, as shown in Fig. 6. Collectively, our data demonstrate that the BFNS effectively and specifically regulated the transcriptional activity of NF-κB which is the mechanism of anti-adhesion that, at least in part, is related to downregulation of the surface proteins in TNF-α-stimulated HUVECs.

In conclusion, the results indicate that BFNS caused significant regulation of TNF-α-induced inflammation, demonstrating a partial molecular basis for the anti-inflammatory properties of the BFNS. This effect was mediated by suppression of iNOS/COX-2 through modulation of NF-κB activity. This study also suggests that the BFNS is useful for treating chronic inflammatory diseases such as cardiovascular disorder, although the constituents of the BFNS were not identified. Isolation and characterization of the constituents that are responsible for the anti-inflammatory activity of BFNS should advance the development of designing functional foods or therapeutic agents.

Acknowledgements

We wish to acknowledge the financial support from the 'Forest Sceince & Technology Projects' (No. S120910L110000) Korea Forest Service (KFS).

References

1. Foteinos G and Xu Q: Immune-mediated mechanisms of endothelial damage in atherosclerosis. Autoimmunity 42: 627-633, 2009.
2. Ross R: Atherosclerosis-an inflammatory disease. N Engl J Med 340: 115-126, 1999.
3. Lui JC, Wong JW, Suen YK, Kwok TT, Fung KP and Kong SK: Cordycepin induced eryptosis in mouse erythrocytes through a Ca^{2+}-dependent pathway without caspase-3 activation. Arch Toxicol 81: 859-865, 2007.
4. Burleigh ME, Babaev VR, Yancey PG, *et al*: Cyclooxygenase-2 promotes early atherosclerotic lesion formation in ApoE-deficient and C57BL/6 mice. J Mol Cell Cardiol 39: 443-452, 2005.
5. Kibbe M, Billiar T and Tzeng E: Inducible nitric oxide synthase and vascular injury. Cardiovasc Res 43; 650-657, 1999.
6. Nachtigal P, Kopecky M, Solichova D, Zdansky P and Semecky V: The changes in the endothelial expression of cell adhesion molecules and iNOS in the vessel wall after the short-term administration of simvastatin in rabbit model of atherosclerosis. J Pharm Pharmacol 57: 197-203, 2005.
7. Cuccurullo C, Mezzetti A and Cipollone F: COX-2 and the vasculature: angel or evil? Curr Hypertens Rep 9: 73-80, 2007.
8. Grassi D, Aggio A, Onori L, *et al*: Tea, flavonoids, and nitric oxide-mediated vascular reactivity. J Nutr 138: 1554S-1560S, 2008.
9. Grassi D, Desideri G, Croce G, Tiberti S, Aggio A and Ferri C: Flavonoids, vascular function and cardiovascular protection. Curr Pharm Des 15: 1072-1084, 2009.
10. Kim HG, Yoon DH, Lee WH, *et al*: *Phellinus linteus* inhibits inflammatory mediators by suppressing redox-based NF-κB and MAPKs activation in lipopolysaccharide-induced RAW 264.7 macrophage. J Ethnopharmacol 114: 307-315, 2007
11. Won KJ, Lee SC, Lee CK, *et al*: Cordycepin attenuates neointimal formation by inhibiting reactive oxygen species-mediated responses in vascular smooth muscle cells in rats. J Pharmacol Sci 109: 403-412, 2009.
12. Kim YS, Ahn Y, Hong MH, *et al*: Curcumin attenuates inflammatory responses of TNF-α-stimulated human endothelial cells. J Cardiovasc Pharmacol 50: 41-49, 2007.

13. Salminen A, Lehtonen M, Suuronen T, Kaarniranta K and Huuskonen J: Terpenoids: natural inhibitors of NF-κB signaling with anti-inflammatory and anticancer potential. Cell Mol Life Sci 65: 2979-2999, 2008.
14. Crespo I, García-Mediavilla MV, Gutiérrez B, Sánchez-Campos S, Tuñón MJ and González-Gallego J: A comparison of the effects of kaempferol and quercetin on cytokine-induced pro-inflammatory status of cultured human endothelial cells. Br J Nutr 100: 968-976. 2008.
15. Godio RP, Fouces R, Gudina EJ and Martin JF: *Agrobacterium tumefaciens*-mediated transformation of the antitumor clavaric acid-producing basidiomycete *Hypholoma sublateritium*. Curr Genet 46: 287-294, 2004.
16. Godio RP, Fouces R and Martin JF: A squalene epoxidase is involved in biosynthesis of both the antitumor compound clavaric acid and sterols in the basidiomycete *H. sublateritium*. Chem Biol 14: 1334-1346, 2007.
17. Godio RP and Martin JF: Modified oxidosqualene cyclases in the formation of bioactive secondary metabolites: biosynthesis of the antitumor clavaric acid. Fungal Genet Biol 46: 232-242, 2009.
18. Kim SN, Son SC, Lee SM, *et al*: Midazolam inhibits proinflammatory mediators in the lipopolysaccharide-activated macrophage. Anesthesiology 105: 105-110, 2006.
19. Hertog MG, Feskens EJ, Hollman PC, Katan MB and Kromhout D: Dietary antioxidant flavonoids and risk of coronary heart disease: the Zutphen Elderly Study. Lancet 342: 1007-1011, 1993.
20. Knekt P, Jarvinen R, Reunanen A and Maatela J: Flavonoid intake and coronary mortality in Finland: a cohort study. BMJ 312: 478-481, 1996.
21. Campbell JH, Efendy JL, Smith NJ and Campbell GR: Molecular basis by which garlic suppresses atherosclerosis. J Nutr 131: 1006S-1009S, 2001.
22. Weitz-Schmidt G, Welzenbach K and Brinkmann V: Statins selectively inhibit leukocyte function antigen-1 by binding to a novel regulatory integrin site. Nat Med 7: 687-692, 2001.
23. Giguère JF and Tremblay MJ: Statin compounds reduce human immunodeficiency virus type 1 replication by preventing the interaction between virion-associated host intercellular adhesion molecule 1 and its natural cell surface ligand LFA-1. J Virol 78: 12062-12065, 2004.
24. Minici F, Miceli F, Tiberi F, *et al*: Ghrelin *in vitro* modulates vasoactive factors in human umbilical vein endothelial cells. Fertil Steril 88: 1158-1166, 2007.
25. Choi JS, Choi YJ, Park SH, Kang JS and Kang YH: Flavones mitigate tumor necrosis factor-alpha-induced adhesion molecule upregulation in cultured human endothelial cells: role of nuclear factor-κB. J Nutr 134: 1013-1019, 2004.